Design and Simulation of an 8-Lead Electrical Capacitance Tomographic System for Flow Imaging

Sidi M. Ahmed Ghaly
Electrical Engineering Department
College of Engineering
Imam Mohammad Ibn Saud Islamic University (IMSIU)
Riyadh, Saudi Arabia
sidiahmedghaly@gmail.com

Khalid Al Snaie
Electrical Engineering Department
College of Engineering
Imam Mohammad Ibn Saud Islamic University (IMSIU)
Riyadh, Saudi Arabia
kalsnaie@imamu.edu.sa

Mohammad Obaidullah Khan
Electrical Engineering Department
College of Engineering
Imam Mohammad Ibn Saud Islamic University (IMSIU)
Riyadh, Saudi Arabia
dearkhan@gmail.com

Mohamed Y. Shalaby
Electrical Engineering Department
College of Engineering
Imam Mohammad Ibn Saud Islamic University (IMSIU)
Riyadh, Saudi Arabia
shalaby88@gmail.com

Majdi Taha Oraiqat
Electrical Engineering Department
College of Engineering
Imam Mohammad Ibn Saud Islamic University (IMSIU)
Riyadh, Saudi Arabia
dr.majdi.taha@gmail.com

Abstract-Electrical Capacitance Tomography (ECT) is a method for determining the dielectric permittivity distribution inside an object from measurements of external capacitance. The technique differs from conventional tomographic methods in which high-resolution images are formed from slices of the material. The measuring electrodes, which are metal plates, must be large enough to give a measurable change in capacitance. The main objective of this paper is the implementation and simulation of 8 external electrode ECT systems in order to increase the quality of reconstructed permittivity images while preserving the simplicity of design and to fulfil the demand for real-time process tomography. A complete sensor model was developed to improve the accuracy of the forward validation, especially the validation of measured data from neighbouring electrodes. A prototype ECT sensor with high sensitivity was designed that can be applied to all materials which have low electrical conductivity. The capacitance between different electrode pairs is calculated for some typical permittivity distributions based on LabVIEW and MATLAB. The obtained capacitance data can be used to reconstruct images. The sensitivity distributions for the ECT sensors with different number of electrodes were analyzed. Preliminary tests were performed and the developed prototype showed good performance. The developed concept contributes to the study and comprehension of the ECT systems that can be used for the monitoring of oil-gas flow.

Keywords-electrical capacitance tomography; permitivity; LabView; simulation; electrode

I. INTRODUCTION

To monitor and diagnose the internal dynamics of a gas/liquid flow mechani1sm system in industrial process, one of the most widely used imaging techniques is the Electrical Capacitance Tomography (ECT) system [1-4] which is an economical, non-interrupting, fast responding imaging scheme. It can generate real-time images, generally with a speed that reaches 100 frames per second. Different experimental outcomes demonstrated that the Water-in-Liquid Ratio (WLR) and Gas Volume Fraction (GVF) in an oil-gas-water flow can be roughly calculated or measured by the ECT with suitable algorithms [5]. To get high-speed imaging along with quantitative measurements of a multi-phase flow system is a challenging demand in petroleum industry hydraulic applications. This can also be used in detecting corrosion, leakage, or to monitor the dynamics of the liquid in the petroleum/gas underwater/underground pipeline network [6-7]. ECT can be employed to investigate the distribution of spatial permittivity within a defined region of interest generally in the interior of a closed pipe. It works on the principle of measuring the capacitances between electrodes located outside of the specimen portion in the region of investigation. Generally, it can be a hollow pipe carrying a liquid or gas. The data achieved from the electrodes are processed to reconstruct the internal image of the pipe. The essential components of a typical ECT system are: a set of multi-electrode sensors, data retrieving or acquisition system, and an image reconstruction system [8-9].

If a sensor uses N electrodes for capacitance measurements, there will be $N(N-1)/2$ unique electrode pairs and thus $N(N-1)/2$ independent capacitance measurements.

$$M = N(N-1)/2 \quad (1)$$

For instance, as illustrated in Figure 1, an 8-electrode sensor needs 28 independent measurements of electrode pairs 1-2, 1-3, ..., 1-8, 2-3, 2-4, ..., 2-8, ..., up to 7-8.

Corresponding author: Sidi M. A. Ghaly

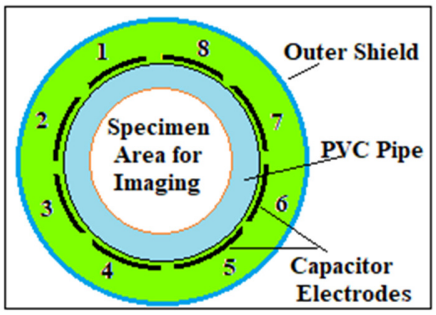

Fig. 1. Cross section of a typical 8-electode sensing system.

Usually the ECT systems use directly the "raw" capacitance data achieved from the sensor to reconstruct images using Linear Back-Projection (LBP), iterative, or neural network algorithms. The LBP algorithm is a commonly used popular method due to its simplicity and high rate of image reconstruction. An LBP image is obtained by superimposing the sensor sensitivity maps (i.e. the sensitivity distributions) for all electrode pairs after weighting by the corresponding measured changes in normalized capacitance [10-11]. This process can be expressed by the mathematical relations given below:

$$X(p) = \frac{\sum_{i=1}^{N-1}\sum_{j=i+1}^{N}\lambda_{ij}S_{ij(p)}}{\sum_{i=1}^{N-1}\sum_{j=i+1}^{N}Sij(p)} \quad (2)$$

$$\lambda_{ij} = \frac{C_{ij}^{m}-C_{ij}^{l}}{C_{ij}^{h}-C_{ij}^{l}} \quad (3)$$

where N is the number of electrodes in an ECT sensor, $X(p)$ is the fraction of high permittivity material in the p^{th} pixel, S is the sensitivity of electrode pair *i-j* at the p^{th} pixel, C_{ij}^{h} and C_{ij}^{l} are the capacitances of the electrode pair *i-j* when the sensor is filled with high and low permittivity materials, and C_{ij}^{m} is the "raw" measured capacitance of electrode pair *i-j*.

This paper focuses on the simulation and design of a prototype ECT sensor, which is used for the measurement of the independent capacitance values. The resolution and sensitivity of an ECT sensor are defined by the number of external electrodes. Therefore, an 8-electrode ECT prototype which is widely used in industrial applications is developed in this paper. The developed prototype is simulated in LabVIEW [12-14] with low and high permittivity materials (air and rod) with permittivity values of 1 and 80 respectively. The developed sensor is used for image reconstruction from the permittivity distribution which is obtained from independent capacitance measurements. A preliminary test is realized with the prototype for the measurement of the independent capacitance values.

II. ELECTRICAL MODELING OF THE ECT SENSOR WITHOUT RADIAL SCREEN

The ECT sensor considered in this article has 8 external electrodes without radial screens as illustrated in Figure 1. These electrodes can be installed with a flexible Printed Circuit Board (PCB) to a greater precision, both in size and in position, than the copper sheet electrodes that use the radial screens. Without radial screens, the external capacitances are to be considered because they are no longer negligible. The measured capacitance of one pair of electrodes C_m, can be modeled as the combination of an internal capacitance C_x, two pipe wall capacitances C_{w1}, C_{w2}, an external capacitance C_{ex}, and two stray capacitances C_{s1}, C_{s2} as illustrated in Figure 2 [15-16].

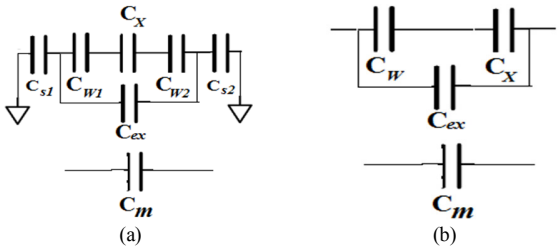

Fig. 2. Electrical model of the 8-electode sensing system without radial screen: a) model with all capacitances, b) simplified model.

Considering Figure 2, the equivalent capacitance C_m can be calculated and measured by the relation:

$$C_m = C_{ex} + \frac{C_w C_x}{C_w + C_x} \quad (4)$$

The unknown capacitances C_{ex}, C_w, and C_x can be found by filling a material of known relative permittivity ε_{r1} into the sensor. This step is repeated with another material of known relative permittivity, say ε_{r2}, e.g. air. Thereby, after finding C_{ex} and C_w, the internal capacitance with any fluid available inside the region of interest in the PVC pipe can be obtained from the raw capacitance measured by (4). Hence, it can be rearranged as [17-18]:

$$C_x = \frac{C_w(C_m - C_{ex})}{C_w - C_m - C_x} \quad (5)$$

III. SIMULATIONS AND RESULTS OF THE ECT SENSOR WITHOUT RADIAL SCREEN

To evaluate the ECT sensor without radial screen model, a cylindrical ECT sensor of 84cm diameter with 8 external electrodes of l0cm length without radial screens (as shown in Figure 1) is employed. It is calibrated with two materials of known permittivity values, air ($\varepsilon = 1$) and a 0.9cm in diameter rod ($\varepsilon = 8$). The prototype simulation data that are the raw capacitance measurements for all electrode pairs, first with the sensor unfilled and then with the rod positioned in the center of the sensor, are obtained by means of the ECT system parameters. These two sets of raw capacitance measurement data with respect to low and high permittivity are shown in Tables I and II respectively. From these measured data, 28 pipe wall capacitances and 28 internal capacitances for air were calculated using (4) and (5). These calculated data show that similar electrode pairs have similar pipe wall capacitance values. All pipe wall capacitances for adjacent electrode pairs are around 400pF, and those of the opposing electrode pairs are around 20pF. As expected, the pipe wall capacitances of adjacent electrode pairs are much larger than those of the other electrode pairs.

TABLE I. RAW CAPACITANCE (PF) DATA MEASURED WITH LOW PERMITTIVITY

Electrode	Detection electrode						
	8	**7**	**6**	**5**	**4**	**3**	**2**
1	362	29	18	11	17	30	370
2	420	29	18	11	17	31	
3	422	30	17	12	18		
4	427	29	18	12			
5	388	30	17				
6	419	30					
7	397						

TABLE II. RAW CAPACITANCE (PF) DATA MEASURED WITH HIGH PERMITTIVITY

Electrode	Detection electrode						
	8	**7**	**6**	**5**	**4**	**3**	**2**
1	420	21	22	24	28	48	407
2	435	21	22	24	29	47	
3	434	22	23	25	30		
4	413	21	22	23			
5	422	21	22				
6	436	21					
7	431						

IV. SIMULATION RESULTS AND DISCUSSION

In an ECT system the number of sensitivity maps equals to the independent capacitance measurements [3]. Each matrix represents the capacitance value of the electrode when the pipe is full with high or low permittivity material. The sensitivity distribution $S_{i,j}(k)$ for the electrode pair *i, j* can be described as:

$$S_{i,j} = \frac{C^m_{i,j} - C^L_{i,j}}{C^h_{i,j} - C^L_{i,j}} \frac{1}{\varepsilon^h - \varepsilon^L} \quad (6)$$

where $C^m_{i,j}$ is the inter electrode capacitance, $C^L_{i,j}$ is the inter electrode capacitance measurement when the sensor area is completely filled with low permittivity material, $C^h_{i,j}$ is the inter electrode capacitance measurement when the sensor is full with high permittivity material, and ε^h and ε^L are the permittivity values for the high and low permittivity materials respectively.

The sensitivity map can be calculated by the sensor, by placing a plastic probe inside the sensing area as shown in Figure 3.

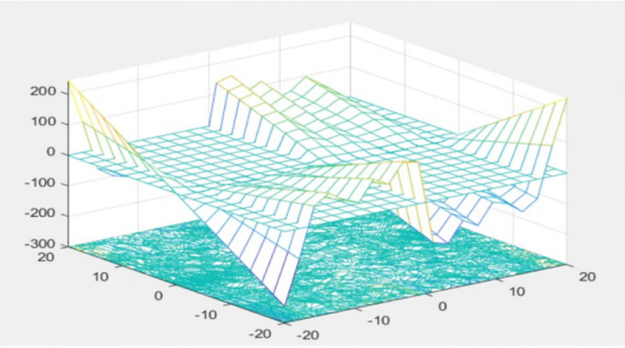

Fig. 3. Total sensitivity map of the 8-electrode ECT system.

The sensitivity matrix defines the change in the measured capacitance between electrodes when the dielectric constant varies inside the sensor and the distribution of the electric field when one electrode is connected to a potential *V* and all the other electrodes are connected to the ground. This shows that the field is strongest close to the exciting electrode and the equi-potential lines inside the sensor. The corresponding lines of the electric field are shown in Figure 4.

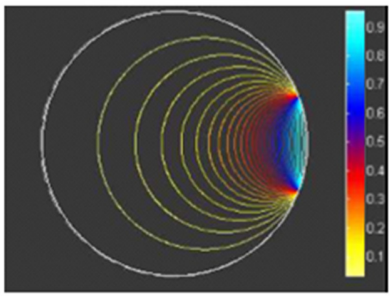

Fig. 4. Illustration of the electric field intensity pattern corresponding to sensitivity.

The change in measured capacitance (sensitivity) between any two electrodes caused by an object with a given permittivity varies depending on where the object is placed (near the walls or the center of the vessel). These data are saved in the sensitivity map text file which is used to develop images of the ECT system by reading the sensitivity map and manipulating the image gray level values accordingly. The field sensitivity distribution of electrode pair *i,j* is defined as [12]:

$$S = E_i.E_j.dA \quad (7)$$

where E_i is the electric field within the specimen sensor when one electrode of the pair *i* is electrified or powered as a source electrode and E_j is the electric field when the electrode *j* is electrified or powered as a source electrode.

To obtain the sensitivity distributions, rotation transformations are further employed in the image domain (the center of the vessel is the center of rotation). Mathematical models have been built to describe such a typical ECT sensor. Using this model, the internal capacitances of two materials with known permittivity (air and rod) and, as appropriate, the pipe wall and/or external capacitances are calculated from the system simulation parameters. The models allow "raw" capacitance measurements to be converted to the internal capacitances before their use in the image reconstruction process. Instead of using the raw simulation data, the equivalent relative permittivity values as defined by:

$$\varepsilon^e_r = \frac{C_x}{C_o} \quad (8)$$

Equation (8) can be used for image reconstruction. For example, a variation of the LBP image reconstruction technique can be used to produce images showing the quantitative distribution. In this technique, the equivalent relative permittivity is expressed by:

$$\varepsilon(p) = \frac{\sum_{i=1}^{N-1}\sum_{j=i+1}^{N} \varepsilon_{ij} S_{ij}(p)}{\sum_{i=1}^{N-1}\sum_{j=i+1}^{N} S_{ij}(p)} \quad (9)$$

$$\varepsilon_{ij} = Cxij/Coij \quad (10)$$

where $\varepsilon(p)$ is the relative permittivity value of the p^{th} pixel, and ε_{ij} is the equivalent relative permittivity of the material between the electrode pair *i,j*.

The permittivity distribution of both materials is obtained as a series of normalized pixels located on a 32×32 square pixel grid. As the sensor cross-section is circular, the simulated contour is projected onto the square grid containing 1024 pixels. Some of the pixels will lie outside the vessel circumference and the image is therefore formed from those pixels that lie inside the vessel. Figure 5 shows the simulated contour for the permittivity distribution of both materials where the circular image is constructed using the available 1024 pixels. A typical frame of the model for image generation and display using LabVIEW is illustrated in Figure 6. The image of the permittivity distribution is represented with an appropriate color scale to indicate the normalized pixel permittivity. The lower permittivity material (air) used is shown in blue, while the higher permittivity material is shown in red.

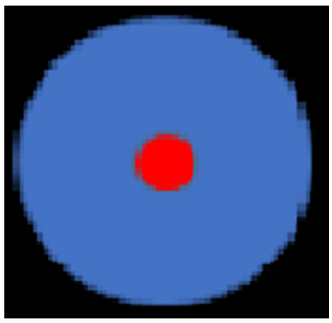

Fig. 5. Illustration of the permittivity distribution represented with an appropriate color scale to indicate the normalized pixel permittivity.

V. DESIGN AND PRELIMENARY TEST

In this part, we present the preliminary measurements obtained with the developed prototype (8-electrode ECT sensor). We conducted tests in the air using a function generator and a digital storage oscilloscope. Gain measurements (normalized capacitance values) of each electrode were carried out and were compared with those found in simulation.

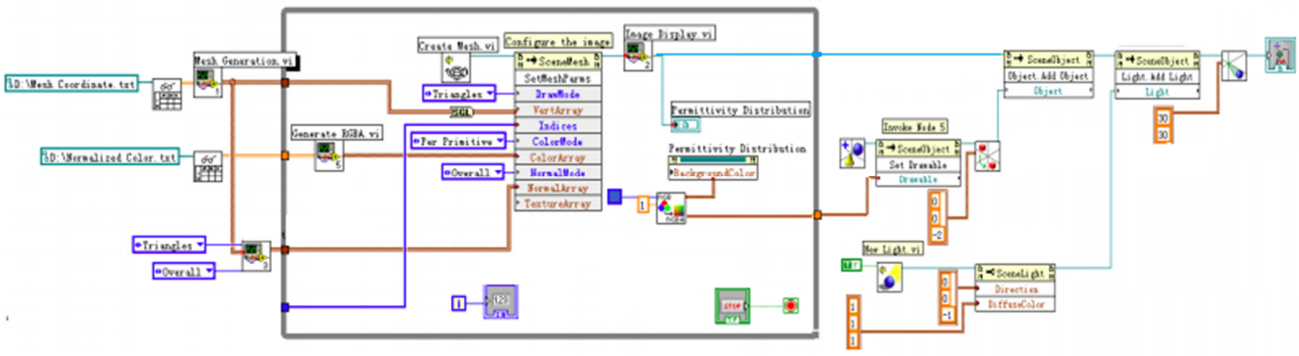

Fig. 6. Diagram of image generation subVI and diagram of image display subVI.

A. Design Requirements

There are some reasons that determine the electrode location. If the tube wall is made up of dielectric material, the electrodes can be installed inside or outside it, but if the wall is conductive there is only one choice to design the electrode location (external electrode), but because the proposed design is employing dielectric material, the electrodes are put outside the pipe, as it is easier to design. The number of electrodes depends on capacitance value, circuit complexity, and data acquisition speed. If more electrodes are used, they provide a better image, but they are difficult to be measured. Mostly, the number of electrodes used is 12 or 8 (in this paper we chose 8). A guard electrode is required to improve the measurement sensitivity, to prevent the electric field from reaching the ground and the end of the measuring electrode. They must be used if the length of measuring electrodes is less than approximately twice the sensor diameter. Finally, it is important to add a discharge resistor. In order to avoid the static charge and the damage of a measuring sensor, the resistor must be connected between each electrode and driven guard and earth. Typically, the value of the resistance is 1MΩ. If the capacitance values of inter-electrodes are around 1pF, an earthed screen is required around the electrodes to avoid unwanted or external signal. A photo of the typically developed prototype is shown in Figure 8.

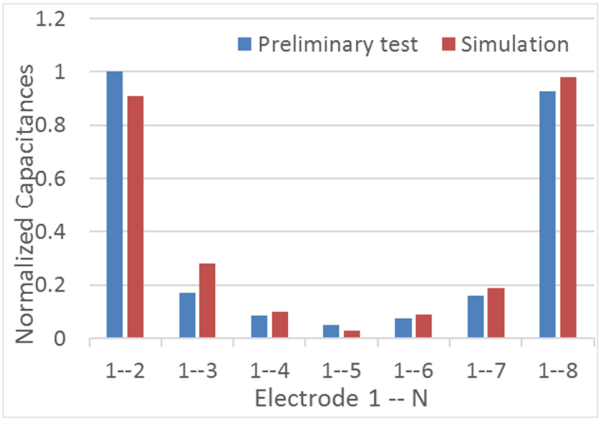

Fig. 7. Normalized capacitance values obtained with preliminary tests and simulations.

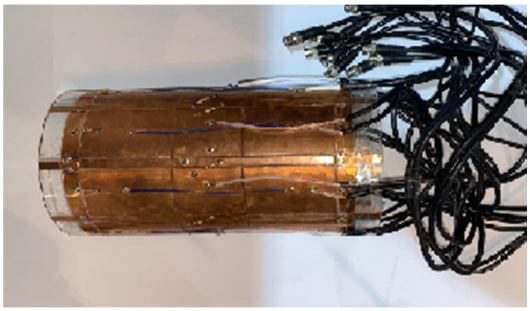

Fig. 8. The developed prototype.

B. Measurements

A photo of the gain measuring of each electrode is presented in Figure 9. For this measurement, each electrode's gain with respect to its neighboring electrode is performed. An input of 10V peak to peak signal is applied from an arbitrary function generator, and the output taken from each and every electrode is measured on digital storage oscilloscope. Since the sensor is symmetrical, there are 3 values of capacitances (C1-2, C1-3, and C1-4) instead of the 28 values whatever the sensor is either filled with a material or not.

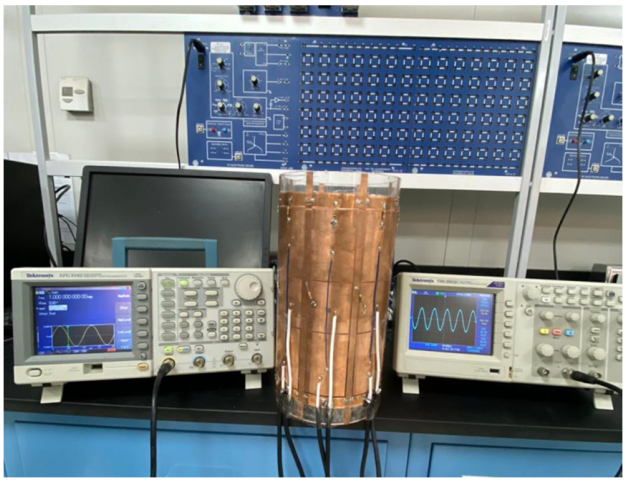

Fig. 9. Illustration of gain measurement of ECT sensor electrodes.

From the results shown in Figure 7, it can be seen that the gain for neighboring electrodes is higher than that of distant electrodes. These values of gain were simulated and measured with the sensor containing air and should be risen if any other material with different dielectric is inside the prototype. Also, an asymmetrical capacitance distribution has observed since the use of a PCB copper foil with the join between electrodes 1 and 8 and small errors in the inter-electrode opening provide large errors in capacitance values between electrodes. Table III gives the designed lengths and measurements.

VI. CONCLUSION AND FUTURE SCOPE

In this paper, the proposed mechanism is illustrated with the help of the powerful software tool LabVIEW. It was shown by the simulations that the internal condition of a closed object can be detected by an internal image taken by means of determining the dielectric permittivity distribution inside from measurements of the external capacitance. Simulations were performed to get the values of capacitance from high and low permittivity for 8 electrode ECT systems and the results illustrate the feasibility of such simulations for generating a 2D image reconstruction.

TABLE III. DESIGNED LENGTHS AND MEASUREMENTS

Type	Length (cm)	Width or diameter (cm)
Pipe	30	15m
Electrodes	6	45
Driven guards	8	45
Earthed screen	4	Along the diameter of the pipe

With the existing technology, image data can be captured at 100 frames per second for a 12-electrode sensor and displayed on-line. For the proposed 8-electrode sensor, this image capture rate is drastically increased up to roughly 200 to 300 frames per second as the number of capacitance measurements is reduced. A typical hardware of the ECT system with 8 outer electrodes covering a cylindrical tube of 15cm diameter with adjustable length, proper resolution and reasonable sensitivity was developed and simulated. This system is being employed with 8 electrodes, so 28 capacitance values were measured, collected, and analyzed in order to get the required image of the fluid flowing inside the tube. In the future, the developed prototype ECT senor can be employed for the monitoring of oil or gas transportation or supply by means of underground/sea pipeline system or in a refinery plant.

ACKNOWLEDGEMENT

This project was funded by the National Plan for Sciences, Technology and Innovation (MAARIFAH) – King Abdulaziz City for Science and Technology – the Kingdom of Saudi Arabia, award number (14-ELE741-08).

REFERENCES

[1] S. M. Huang, A. B. Plaskowski, C. G. Xie, and M. S. Beck, "Tomographic imaging of two-component flow using capacitance sensors," *Journal of Physics E: Scientific Instruments*, vol. 22, no. 3, pp. 173–177, Mar. 1989, https://doi.org/10.1088/0022-3735/22/3/009.

[2] M. S. Beck and R. A. Williams, "Process tomography: a European innovation and its applications," *Measurement Science and Technology*, vol. 7, no. 3, pp. 215–224, Mar. 1996, https://doi.org/10.1088/0957-0233/7/3/002.

[3] T. Dyakowski *et al.*, "Imaging nylon polymerisation processes by applying electrical tomography," *Chemical Engineering Journal*, vol. 77, no. 1, pp. 105–109, Apr. 2000, https://doi.org/10.1016/S1385-8947(99)00132-1.

[4] M. S. Beck, T. Dyakowski, and R. A. Williams, "Process tomography - the state of the art," *Transactions of the Institute of Measurement and Control*, vol. 20, no. 4, pp. 163–177, Oct. 1998, https://doi.org/10.1177/014233129802000402.

[5] W. Q. Yang, "Calibration of capacitance tomography systems: a new method for setting system measurement range," *Measurement Science and Technology*, vol. 7, no. 6, pp. L863–L867, Jun. 1996, https://doi.org/10.1088/0957-0233/7/6/001.

[6] S. M. Huang, C. G. Xie, M. S. Beck, R. Thorn, and D. Snowden, "Design of sensor electronics for electrical capacitance tomography," *IEE Proceedings G (Circuits, Devices and Systems)*, vol. 139, no. 1, pp. 83–88, Feb. 1992, https://doi.org/10.1049/ip-g-2.1992.0014.

[7] Ø. Isaksen, "A review of reconstruction techniques for capacitance tomography," *Measurement Science and Technology*, vol. 7, no. 3, pp. 325–337, Mar. 1996, https://doi.org/10.1088/0957-0233/7/3/013.

[8] W. Q. Yang, D. M. Spink, T. A. York, and H. McCann, "An image-reconstruction algorithm based on Landweber\textquotesingles iteration method for electrical-capacitance tomography," *Measurement Science and Technology*, vol. 10, no. 11, pp. 1065–1069, Sep. 1999, https://doi.org/10.1088/0957-0233/10/11/315.

[9] Z. Fan and R. X. Gao, "Enhancement of Measurement Efficiency for Electrical Capacitance Tomography," *IEEE Transactions on Instrumentation and Measurement*, vol. 60, no. 5, pp. 1699–1708, May 2011, https://doi.org/10.1109/TIM.2011.2113010.

[10] W. Warsito, Q. Marashdeh, and L.-S. Fan, "Electrical Capacitance Volume Tomography," *IEEE Sensors Journal*, vol. 7, no. 4, pp. 525–535, Apr. 2007, https://doi.org/10.1109/JSEN.2007.891952.

[11] Q. Marashdeh, F. Wang, L.-S. Fan, and W. Warsito, "Velocity Measurement of Multi-Phase flows Based on Electrical Capacitance Volume Tomography," in *2007 IEEE SENSORS*, Atlanta, GA, USA, Oct. 2007, pp. 1017–1019, https://doi.org/10.1109/ICSENS.2007.4388577.

[12] F. Alorifi, S. M. A. Ghaly, M. Y. Shalaby, M. A. Ali, and M. O. Khan, "Analysis and Detection of a Target Gas System Based on TDLAS & LabVIEW," *Engineering, Technology & Applied Science Research*, vol. 9, no. 3, pp. 4196–4199, Jun. 2019, https://doi.org/10.48084/etasr.2736.

[13] S. M. A. Ghaly, "LabVIEW Based Implementation of Resistive Temperature Detector Linearization Techniques," *Engineering, Technology & Applied Science Research*, vol. 9, no. 4, pp. 4530–4533, Aug. 2019, https://doi.org/10.48084/etasr.2894.

[14] S. M. A. Ghaly, M. O. Khan, S. O. E. Mehdi, M. Al-Awad, M. A. Ali, and K. A. Al-Snaie, "Implementation of a Broad Range Smart Temperature Measurement System using Auto-Selected Multi-Sensor Core in LabVIEW Environment," *Engineering, Technology & Applied Science Research*, vol. 9, no. 4, pp. 4511–4515, Aug. 2019, https://doi.org/10.48084/etasr.2896.

[15] Z. Cao, L. Xu, and H. Wang, "Image reconstruction technique of electrical capacitance tomography for low-contrast dielectrics using Calderon\textquotesingles method," *Measurement Science and Technology*, vol. 20, no. 10, Sep. 2009, Art. no. 104027, https://doi.org/10.1088/0957-0233/20/10/104027.

[16] M. Baidillah, W. Warsito, and M. Mukhlisin, "The Optimum Design of 3D Sensor for Electrical Capacitance Volume-Tomography (ECVT)," *Jurnal Matematika dan Sains*, vol. 16, no. 3, pp. 123–128, Dec. 2011.

[17] M. R. Baidillah, M. Mukhlisin, and W. P. Taruno, "Comparisons of sensor geometries for electrical capacitance volume tomography," *International Journal of Innovative Computing, Information and Control*, vol. 9, no. 11, pp. 4447–4457, Nov. 2013.

[18] S. M. A. Ghaly and S. Al-Sowayan, "A High B1 Field Homogeneity Generation Using Free Element Elliptical Four-Coil System," *American Journal of Applied Sciences*, vol. 11, no. 4, pp. 534-540, Feb. 2014, https://doi.org/10.3844/ajassp.2014.534.540.